Article

Not peer-reviewed version

From Waste to Technological Products: Bioplastics Production from Proteins Extracted from Black Soldier Fly

Alessia Di Pasquale , Marina Zoccola * , Ashish Mohod , Giulia Dalla Fontana , Anastasia Anceschi , Sara Dalle Vacche

Posted Date: 6 May 2025

doi: 10.20944/preprints202505.0100.v1

Keywords: bioplastics; Black Soldier Fly; proteins; polyvinyl alcohol; circular economy; biofactory; high-value products

 doi:10.20944/preprints202505.0100.v1

Article

From Waste to Technological Products: Bioplastics Production from Proteins Extracted from Black Soldier Fly

Alessia Di Pasquale [1], Marina Zoccola [2,*], Ashish Mohod [2], Giulia Dalla Fontana [2], Anastasia Anceschi [2] and Sara Dalle Vacche [1]

[1] Department of Applied Science and Technology, Politecnico di Torino, Corso Duca degli Abruzzi 24, 10129 Torino, Italy

[2] CNR-STIIMA, Italian National Research Council, Institute of Intelligent Industrial Technologies and Systems for Advanced Manufacturing, Corso G. Pella 16, 13900 Biella, Italy

* Correspondence: marina.zoccola@cnr.it

Abstract: The need to find sustainable solutions to conventional plastics has driven research into alternative materials, including bioplastics, which represent a promising option for reducing pollution and enhancing the value of renewable resources. In this study, bioplastics made from polyvinyl alcohol (PVA) and proteins extracted from the larvae of Black Soldier Fly (BSF), an insect capable of converting organic waste into high-value biomass, were produced and characterized. The proteins were obtained by hydrolysis of defatted BSF larvae with superheated water, avoiding harsh chemical reagents. Next, polymer films were fabricated by mixing PVA and hydrolyzed BSF proteins in different proportions and analyzed for morphological, physical-chemical, mechanical and biodegradability characteristics. The results obtained show that as the BSF protein content increases, the films show a reduction in thermal stability and mechanical strength, which makes the films more brittle and flexible, and they exhibit higher biodegradability, correlated with higher wettability, solubility and ability to absorb moisture. This research highlights the value of using organic waste-fed insects as a resource for bioplastic production, offering an alternative to traditional polymers and contributing to the transition to sustainable materials.

Keywords: bioplastics; Black Soldier Fly; proteins; polyvinyl alcohol; circular economy; biofactory; high-value products

1. Introduction

Hermetia illucens, also known as Black Soldier Fly, is an insect of the order Diptera and the family Stratiomyidae. This species is native to South America, but is currently widespread on a cosmopolitan level, due to its ability to adapt to many different environments and food sources [1]. The life cycle of BSF consists of four main stages, the first stage being eggs laid near decomposing organic material. The larvae then come out of the eggs and grow rapidly, accumulating body mass. When they reach maturity, they become first prepupae, where they stop feeding and their skin hardens, and immediately after pupae, where they undergo the metamorphosis into winged adults, which concentrate exclusively on reproduction [2]. BSF larvae have the potential to bioconvert a large variety of organic substrates in their body mass and they can be used in waste management requiring a relatively low amount of water, land and energy to be reared [3–5].

As insects are 'farmed animals' [6], the EU legislation does not allow to feed them with organic waste [7]. However, to implement the circularity level of the EU insect sector and help it to reach its full potential, the International Platform of Insects for Food and Feed [8] has identified as a key research priority the diversification of the allowed growing substrates. Moreover, around the world, such legislation does not apply and BSF larvae are a very valuable tool for waste management [9–13].

 doi:10.20944/preprints202505.0100.v1

This process has several advantages compared to traditional organic waste treatment strategies. It could make a very meaningful contribution to meeting several of the UN Sustainable Development Goals (SDGs) for 2030 and thereafter.

The present work focused on extracting proteins from BSF larvae raised on food scraps and their use for technological purposes for bioplastic production.

The European Union generated 59.2 million tonnes of food waste in 2022, corresponding to around 132 kg per inhabitant [14]. The recycling of food waste to produce commercial products and energy is fast picking up in the scientific community as a sustainable option [15]. Food waste is characterized by a variable chemical composition depending on its origin of production, while feeding insects with food waste allows for concentrating the waste in their body mass, which can be biorefined, obtaining fat, protein and chitin [16].

After the grease extraction, proteins can be extracted from the insect body mass using strong bases, in particular NaOH, which is the most widespread and widely established method [17,18], or enzymes [1,19].

In this study, to extract proteins from BSF larvae, superheated water at a temperature of 160°C corresponding to a pressure of 4.5 bar was used, which offers the advantages of being an environmentally sustainable process, not requiring complex and expensive purification steps, as well as sterilizing the material and ensuring a safe protein end product.

Superheated water is defined as liquid water under pressure at a temperature between 100 °C (boiling temperature at atmospheric pressure) and 374°C (critical water temperature) [20]. As far as the protein is concerned, superheated water has been used to obtain keratins from wool and feathers [21–23] and to extract protein from insects to obtain natural dyes [24] or to remove proteins and isolate chitin from BSF exuviae [25].

In this study, the proteins extracted from BSF with superheated water were blended with PVA for bioplastic production to overcome the disadvantages of the protein's fragile structure and poor mechanical properties [26]. PVA was chosen because it is a hydrophilic polymer, water soluble, biodegradable, with the good film-forming ability [27] and compatible with proteins in film production [28–30].

The bioplastic production from insect larvae feeding on food waste is a solution within a circular economy and reduces dependence on polymers from fossil sources.

Bioplastics are characterized by their derivation from renewable resources or because they are biodegradable, which means they can degrade in natural environments or under specific industrial conditions [31,32]. In the case of insect proteins, both requirements are met.

Biodegradable polymers are transformed into water, carbon dioxide, methane or biomass through biological processes, making them particularly useful for applications such as single-use materials where end-of-life management is challenging [33]. In addition, this type of bioplastics could find application in agriculture where traditional plastics, such as low-density polyethylene (LDPE), are widely used as mulching films and although appreciated for their low cost and good mechanical and optical performance, during the degradation process, they reduce into fragments that have to be removed [34].

On the other hand, bioplastics from proteins are designed not only to degrade completely without leaving harmful residues but also to release carbon and organic nitrogen that fertilize the soil and support crop growth [35,36].

In this study, bioplastics were obtained from BSF larvae proteins extracted by a green method using only water under pressure and mixed with PVA in different proportions using water as a common solvent. The bioplastics were characterized by chemical (spectroscopy in the medium infrared - FTIR) thermal, mechanical, and morphological analyses, and parameters such as water solubility, moisture absorption, contact angle, and biodegradability in soil were measured aiming to characterize the different films and direct them towards specific uses.

2. Materials and Methods

 doi:10.20944/preprints202505.0100.v1

2.1. Materials

The proteins were extracted from BSF larvae reared at the experimental center of the Department of Zootechnical Sciences of the University of Turin in Carmagnola (Turin), in a climate chamber with controlled temperature and humidity (29 ± 0.5°C, relative humidity 60 ± 5%) and constant ventilation. PVA was supplied by the company F.lli Citterio S.p.A. (Monza- Italy) in filament form. Distilled water was prepared using the Millipore apparatus. All the other reagents were of analytical grade and were purchased from Sigma-Aldrich.

2.2. Methods

2.2.1. BSF Larvae and PVA Preparation

BSF larvae at the last larval age were dried (see Figure 1), washed 3 times in deionized water, further dried at 55 °C for 24 h and finely ground in a blender.

The larval powder was then extracted in a Soxhlet apparatus for 4 h using hexane as a solvent to remove larval fat. From the defatted larvae, the proteins were extracted. The PVA yarn was extracted in a Soxhlet apparatus for 4 h using petroleum ether as a solvent to remove fats and finishing products.

Figure 1. Dried BSF larvae.

2.2.2. Protein Extraction from BSF Larvae and Their Characterization

Superheated water was used for protein extraction in a laboratory reactor (Amar Equipment), which had a capacity of 5 l and was equipped with a magnetically coupled stirrer driving a paddle turbine. Specifically, 50 g of ground and defatted BSF larvae were suspended in 1 l of distilled water, and hydrolysis was conducted for 1 h and under stirring at 400 rpm.

Three hydrolysis tests were carried out: the first at a temperature of 160 °C (pressure 4.5 bar), the second at the same temperature of 160 °C and it was preceded by pretreatment with HCl (2N) for 24 h at room temperature and material to liquor ratio of 1/10 in a conical flask under stirring of 130 shakes/min. After filtration on wire mesh, neutralization with ammonia and rinsing with tap water, the solid part was hydrolyzed in an autoclave. The third test was conducted on grounded and defatted BSF larvae at a temperature of 180 °C corresponding to a pressure of 10 bar.

Each hydrolysate was filtered on a wire mesh, and the protein-rich liquid was further centrifuged at 8000 rpm for 15 min to remove precipitated solid material.

To determine the protein concentration, 10 ml from each liquid extract were dried in an oven at 105 °C for 4 h, and the dry weight was measured.

By measuring the final volume of each extract, the extraction yield was calculated using the formula:

$$Extraction\ yield\ (\%) = \frac{Wf}{Wi} \times 100 \quad (1)$$

 doi:10.20944/preprints202505.0100.v1

where:

wf: dry weight of hydrolyzed proteins

wi: dry weight of defatted BSF larvae before hydrolysis

2.2.3. Preparation of PVA/BSF Protein Blend Films

The protein hydrolysate from BSF larvae obtained from superheated hydrolysis at 160°C for 1 h, having a protein concentration of 21 g/l, was placed in a flask in a thermostated bath at 65°C for 1 h under stirring (130 shakes/min). PVA filament in water was treated under the same conditions and dissolved completely. The two solutions were mixed in the proportions PVA/BSF protein % w/w 100/0, 90/10, 70/30, 50/50, 30/70, 10/90 and 100/0 in a volume of 10 ml for each blend. The solutions at the different PVA/BSF protein concentrations were further mixed in a thermostatically controlled bath at 65 °C for 1 h under stirring (130 shaking/min) and then cast onto polyester plates and allowed to dry at room temperature for 48 h until complete water evaporation.

2.3. Characterization of PVA/BSF Protein Blend Films and BSF Protein Hydrolyzates

FT-IR Spectroscopy

BSF larvae, liquid and solid fractions after hydrolysis, PVA/BSF protein films and PVA/BSF films after biodegradation in soil were characterized by FT-IR spectroscopy in ATR (Attenuated Total Reflectance) mode with a diamond crystal. The Thermo Nexus spectrometer (Nicolet) instrumentation was used, and the spectra were processed with Omnic software. Spectra were acquired with 64 scans in the wavenumber range 4000-650 cm^{-1} with resolution 4 cm^{-1} and gain 8.

2.4. Characterization of PVA/BSF Protein Blend Films

2.4.1. Thermal Behaviour

Thermal characteristics were determined by Differential Scanning Calorimetry (DSC) and Thermogravimetric Analysis (TGA). A DSC 821e Mettler Toledo equipment was used, and data was processed using STARe SW 9.30 software. 2- 3 mg sample was inserted in an aluminium crucible and heated from 50 to 400 °C at a heating rate of 5 °C /min under a 10 ml/min nitrogen flow.

The relative crystallinity degree of PVA in the different films was calculated for reference to the pure PVA films by measuring the area of the melting peak corresponding to the melting enthalpy (ΔH_f) through the formula:

$$X_c(\%) = \frac{\Delta H_f}{\left(\frac{\%PVA}{100}\right) \times \Delta H_{f,100\%PVA}} \times 100 \quad (2)$$

where

X_c: relative crystallinity degree of PVA in films at different PVA concentration

$\Delta H_{f100\%PVA}$: PVA melting peak area in pure PVA sample

ΔH_f: PVA melting peak area in samples at different PVA concentration

For TGA, thermograms were acquired using a TGA/DSC Mettler Toledo and processed using STARe SW 9.30. The software allows us to obtain both TGA curves and DTG derivatives. The analyses were carried out in 5-10 mg samples over a temperature range from 30 °C to 700 °C, with a constant heating rate of 10°C/min under 70 ml/min nitrogen flow.

2.4.2. Solubility in Water

Films were dried in an oven at 50 °C until constant weight and then immersed in 50 ml distilled water at room temperature for 24 h under shaking (130 shaking/min). The films were then filtered under a vacuum to recover solid parts and dried at 50 °C until constant weight, as reported by Gontard et al. [37]. Each experiment was repeated in triplicate.

Solubility in water was calculated using the formula:

 doi:10.20944/preprints202505.0100.v1

$$Solubility\ in\ water(\%) = \frac{w_i - w_f}{w_i} * 100 \quad (3)$$

where:

w_i: initial sample dry weight

w_f; final sample dry weight

2.4.3. Water Uptake

PVA/BSF protein films were dried in an oven at 50 °C and then conditioned in a room at 20 °C and 65 % of relative humidity for at least 24 h before weighing each sample every hour for 8 hours and then after 24 hours, as reported by Patrucco et al. [38].

Experiments were conducted in triplicate and water uptake was calculated by the formula:

$$Water\ Uptake(\%\ w/w) = \frac{W_f - W_i}{W_i} * 100 \quad (4)$$

where:

W_i: initial dry weight

W_f: weight after *n hours in a conditioned environment

*n: 1, 2, 3, 4, 5, 6, 7, 8, 24 h

2.4.4. Morphological Characterization

Scanning Electron Microscopy (SEM) analysis was carried out on Zeiss EVO 10 equipment using SmartSEM software with 20 μA of the current probe, an acceleration voltage of 20 kV, and 30 mm working distance. PVA/ BSF protein films were mounted on aluminium stubs and made to adhere using a double-sided adhesive tape. Before analysis, samples were sputter coated with a thin gold layer under a rarefied argon atmosphere.

2.4.5. Tensile Behaviour

Films were cut into strips 2 mm width x 25 mm length and were tested with a dynamometer Zwick Roell Z005 in a conditioned atmosphere at the constant rate of 10 mm/min according to the EN-ISO 5079 standard [39]. Data were processed using TestXPer III software. At least three measurements were carried out for each sample and tensile strength, modulus and elongation at break were reported. The thickness of each film was measured using a digital comparator (Fowler).

2.4.6. Contact Angle

For the contact angle measurement, an optical goniometer EasyDrop model from Kru¨ss (Germany) was used with the sessile drop method. A 10.5 μl milliQ water drop was deposited on the film surface with a syringe and the angle formed by each film surface and the drop profile was measured. 8 measurements were performed on each film to obtain the mean and standard deviation.

2.5. Biodegradation Testing in Soil

PVA/ hydrolyzed BSF protein films were dried at 50 °C, put in nylon mesh bags and buried under natural soil in a pot as reported by Bhavsar et al. [35]. The soil was kept moist by periodic irrigation, and samples were removed after 10/20/30/60/90 days and dried again at 50°C.

The determination of biodegradability in soil was calculated by the following formula:

$$Weight\ loss[\%\ w/w] = \frac{W_i - W_f}{W_i} \text{ x100 (5)}$$

where:

W_i: initial dry weight

W_f: dry weight after *n dyes of burial in soil

*n: 10/20/30/60/90 days

FTIR spectra were acquired on each film after soil removal.

 doi:10.20944/preprints202505.0100.v1

3. Results

3.1. Characterization of BSF Larvae and BSF Protein Extracts

The extraction hydrolysis yields referred to the dry weight of the defatted BSF larvae were 45.51% w/w for the trial carried out at 160 °C, 13.77% w/w for the trial at 160 °C after pretreatment with HCl, and 45.96 % w/w for the trial at 180 °C. The time was always 1 h and the solvent was pressurized water, which offers the advantages of sterilizing the material and obtaining the extracts directly in water, avoiding costly and time-consuming purification processes.

The low yield of the process preceded by HCl pretreatment is presumably due to the loss of material during pretreatment, neutralization, and rinses, while the similar extraction yield of the 160 °C and 180 °C processes suggests that the temperature of 160 °C for 1 h is sufficient to extract the proteins and is not necessary to increase temperature and consume more energy.

The FT-IR spectra of the three extracts are shown in Figure 2. They have similar absorptions mainly attributable to the presence of proteins. In fact, the peaks of Amide I at about 1650 cm^{-1} (C=O stretching), Amide II at about 1550 cm^{-1} (C=N stretching and N-H bending) and Amide III at about 1230 cm^{-1} (C-N stretching and N-H bending) are present and the peaks of Amide A at 3270 cm^{-1} and Amide b at 2930 cm^{-1} representing N-H stretching and C-H stretching respectively, are also visible [40].

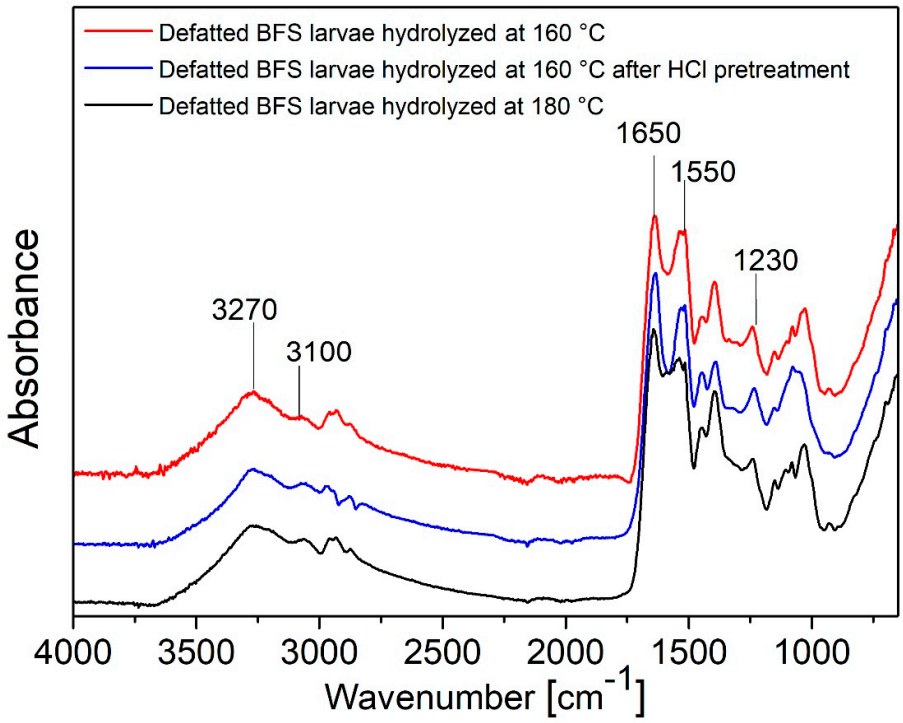

Figure 2. FTIR spectra of dried protein extracted from defatted BSF larvae at 160 °C, 160 °C after HCl pretreatment and 180 °C.

As observed in Figure 3, in BSF larvae spectra, there are present peaks from lipids at 2954 cm^{-1} (-CH_3 asymmetrical stretch), at 2922 and 2853 cm^{-1} (symmetrical and asymmetrical stretching of -CH_2), at 1743 cm^{-1} (-C=O stretch), and at 1713 cm^{-1} corresponding to carbonyl absorption [41]. All these absorptions are not present in the hydrolysate as grease was removed by extraction with hexane.

 doi:10.20944/preprints202505.0100.v1

Moreover, in the solid part remaining as a deposit not extracted with the superheated water, there is a strong absorption due mainly to the mineral fraction with the characteristic peak of calcite ($CaCO_3$) at 1030 cm^{-1} imputable to symmetric CO_3 stretching [42] while the absorptions of the chitin present in the larvae overlap with non-solubilized protein and the inorganic parts absorptions [25]. Finally, as previously stated, protein peaks referable to amides are clearly visible in the dried extract.

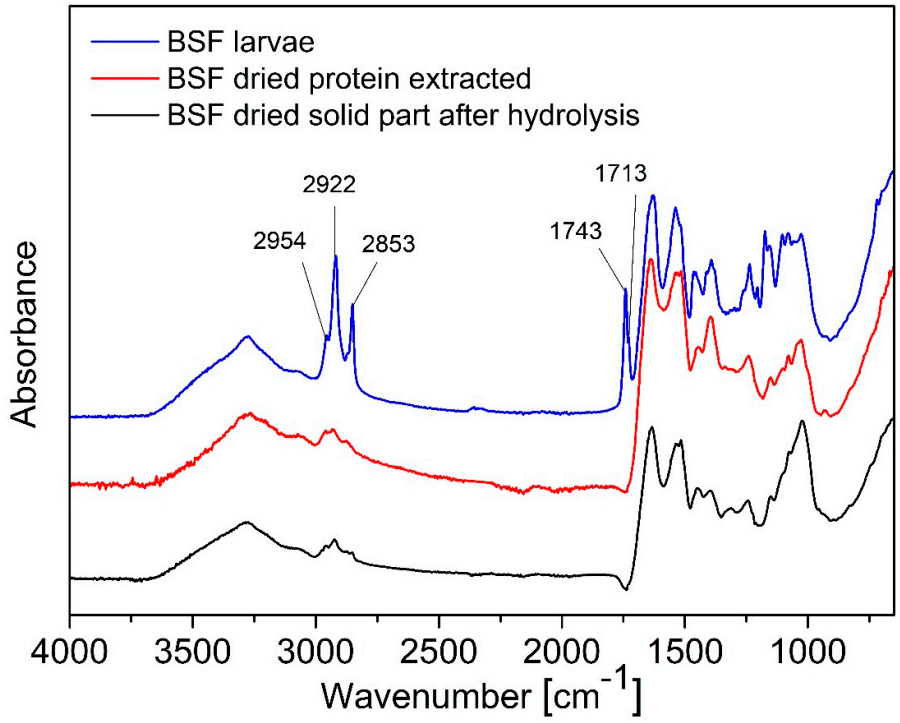

Figure 3. FTIR spectra of BSF larvae, BSF dried proteins extracted, BSF dried solid part after hydrolysis.

3.2. Characterization of PVA/BSF Protein Blend Films

All PVA/BSF protein blends showed good film-forming ability except for the higher amount of protein blends (10/90 and 0/100 % w/w), which produced brittle films hard to peel from the cast.

The films show visual properties influenced by their composition. They generally appear quite smooth with an even material distribution. However, in samples with a high concentration of protein, surface irregularities emerge. Regarding coloration, films with a higher percentage of PVA appear more transparent, while those with a high protein composition are more opaque and brownish in colour (see Figure 4).

Figure 4. The visual appearance of PVA/ BSF proteins films in % w/w 100/0, 90/10, 70/30, 50/50, 30/70, 10/90 and 0/100 from left to right.

3.3. FT-IR Spectroscopy

 doi:10.20944/preprints202505.0100.v1

The PVA/ BSF protein films at different compositions were characterized by FT-IR spectroscopy, as shown in Figure 5.

In films composed exclusively of PVA, the band located at about 3300 cm-¹ appears broad and intense, highlighting intra- and intermolecular hydrogen bonds between the O-H groups of PVA. By increasing the protein concentration, this band broadens and reduces its intensity. This behaviour is attributed to the interference of the N-H bond protein stretching and the formation of new hydrogen bonds between PVA and BSF proteins. Finally, in samples with low PVA amounts, the band becomes less defined, indicating the predominance of N-H stretching from BSF proteins.

In contrast, the Amide I band at about 1650 cm-¹ and Amide II bands at about 1550 cm-¹ are characteristic signals of proteins and increase with increasing BSF protein fraction in films [43].

Moreover, an intense peak at about 1100 cm-¹ can be seen in the films with higher amounts of PVA, representing symmetric C–C stretching mode or some stretching of the C–O bonds. This absorption is strongly associated with PVA crystallinity as referred to by Mansur et al. [44]. In blend films, this absorption reduces intensity as the protein content increases, showing a partial decrease in PVA content and its crystallinity.

In conclusion, FT-IR analysis highlights the compatibility between PVA and BSF proteins in films due to noncovalent interactions, particularly hydrogen bonds.

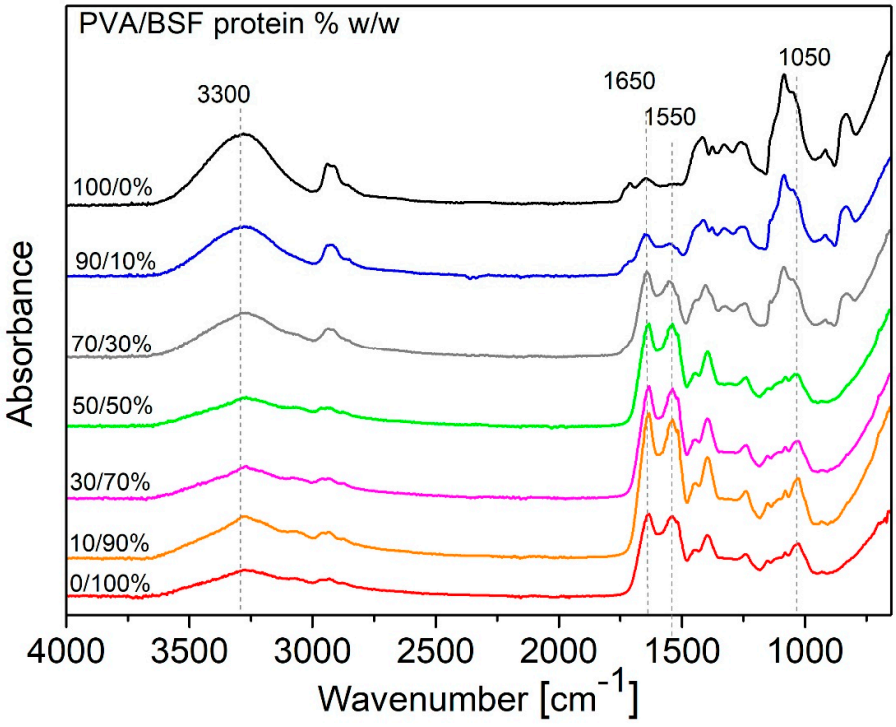

Figure 5. FTIR spectra of PVA/BSF proteins films in % w/w 100/0, 90/10, 70/30, 50/50, 30/70, 10/90 and 0/100.

3.4. Thermal Behaviour

The DSC curves of the films at different percentages of PVA/ BSF protein (see Figure 6) show a first endothermic peak of around 80°C attributable to water evaporation and a second endothermic peak at around 212°C for pure PVA representing the melting point of the crystalline regions of PVA [45,46].

 doi:10.20944/preprints202505.0100.v1

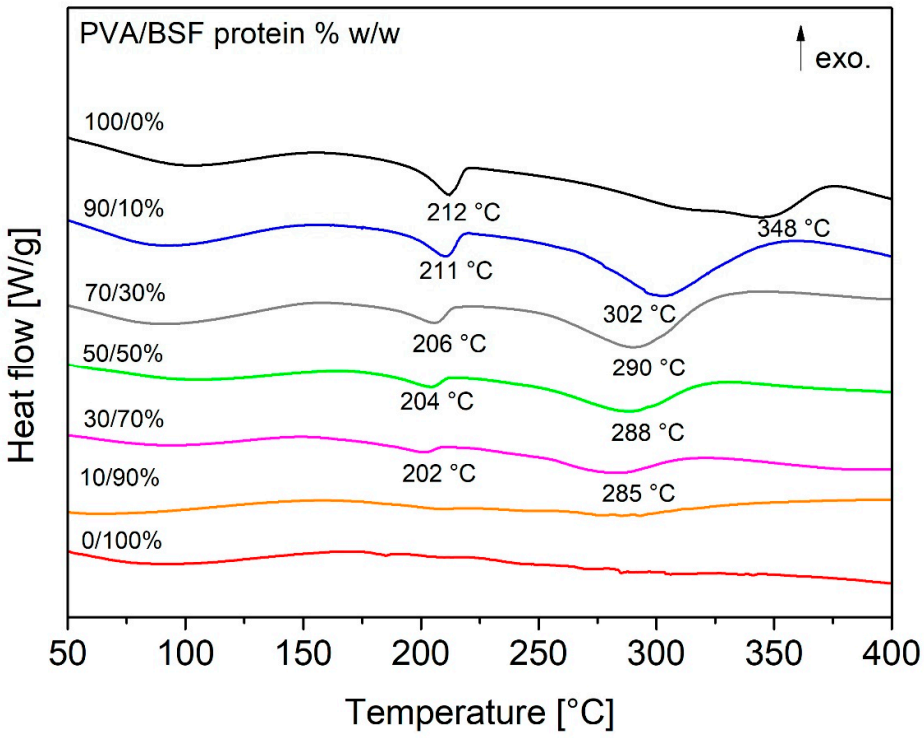

Figure 6. DSC traces of PVA/BSF protein films at different concentration.

As the protein concentration increases in different films, there is a progressive decrease in the intensity of this peak correlated with the decrease in the crystallinity of PVA, while its temperature undergoes a progressive reduction from 212 °C of the pure PVA film to 201 °C of the PVA/ BSF protein 30/70% w/w film. The percentage of crystallinity relative to the pure PVA sample of the different samples (except the PVA/BSF protein 10/90% w/w sample due to the absence of a significant crystalline phase) was calculated using the formula 2, and the results are shown in Table 1.

Table 1. PVA relative crystallinity degree and melting enthalpy area for its calculation.

PVA/BSF protein (% w/w)	ΔH_f [J/g]	X_c [%]
100/0	4.3552	100
90/10	3.8424	98.25
70/30	2.5645	84.32
50/50	1.7062	78.18
30/70	0.2203	71.18

A progressive reduction in the relative crystallinity of PVA can be seen as the protein fraction increases, reaching the value of 71.18 % in the 30 % PVA sample. This trend can be attributed to interactions between PVA and BSF proteins, which insert between PVA polymer chains, limiting the PVA crystallization process, favoring a prevalence of amorphous regions within the films and affecting their physical and mechanical properties.

Finally, an additional endothermic event emerges in the DSC traces at higher temperatures that could be associated with protein degradation.

The results of thermogravimetric analysis of PVA/ BSF protein films at different concentrations are shown in Figure 7 and summarized in Table 2.

 doi:10.20944/preprints202505.0100.v1

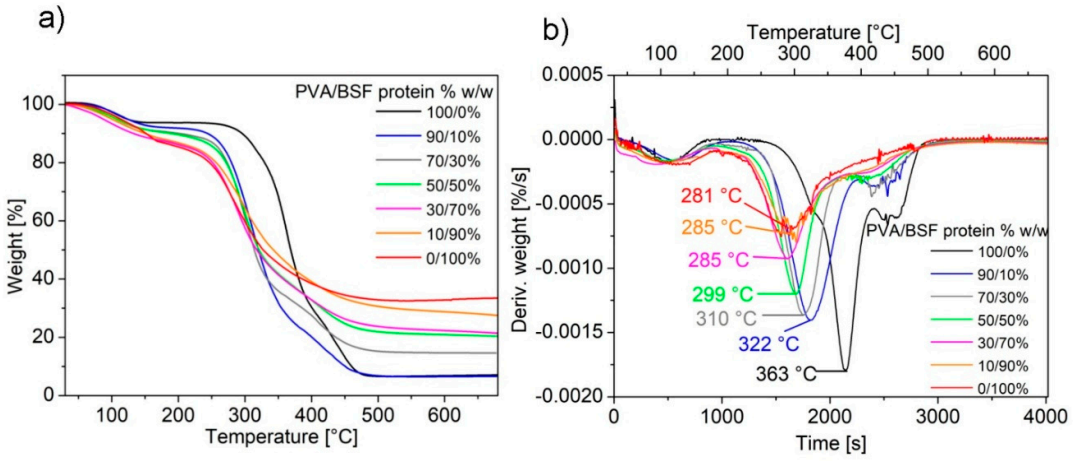

Figure 7. TGA traces of PVA/BSF protein films at different concentrations (a) and their first derivatives (b).

TGA traces show an initial weight loss due to water evaporation at temperatures below 120 °C and degradation at a T_{onset} that increases with increasing PVA concentration. This behaviour indicates that PVA promotes a stabilizing effect on the polymer matrix, delaying the T_{onset} of thermal decomposition. In particular, the pure protein film exhibits the lowest temperature of 128.1 °C, consistent with the nature of proteins, which tend to degrade due to denaturation of their structures and disruption of intermolecular bonds. Minimal addition of PVA leads to a significant increase in T_{onset}, which reaches 235.7 °C, highlighting the strong stabilizing impact of PVA. With increasing PVA concentration, a gradual T_{onset} increase is observed until it reaches 333.4 °C in the case of pure PVA.

The final residue shown in Table 2 was calculated as a function of the dry weight of the films, excluding the part of the curve where the weight loss is due to water evaporation.

The final residue of 35.5% w/w in the pure protein sample indicates the BSF protein's tendency to leave a significant carbonaceous residue after thermal decomposition rather than decomposing completely into volatile compounds. The residue progressively decreases with the addition of PVA, showing that pyrolysis is increasingly complete due to the PVA contribution. A final residue of 7.4% w/w is achieved in pure PVA samples.

Finally, from the DTG (Derivative Thermogravimetry) curves, the peak temperature represents when the material decomposes at the maximum rate. In the pure protein sample, the DTG peak occurs at 280.8 °C, corresponding to the degradation of polypeptide chains [47]. As PVA increases in films, an increasingly pronounced shift of the peak toward higher temperatures is observed until it reaches 362.5 °C with pure PVA, confirming the stabilizing PVA impact.

Table 2. TGA parameters of PVA/BSF protein films at different concentrations.

PVA/BSF protein [% w/w]	T_{onset} [°C]	T_{peak} [°C]	Residue [% w/w]
100/0	333.4	362.5	7.4
90/10	275.9	310.1	6.9
70/30	268.1	299.1	15.5
50/50	260.3	299.4	21.6
30/70	241.8	284.6	23.3
10/90	235.7	284.7	29.4
0/100	128.1	280.8	35.5

3.5. Solubility in Water

 doi:10.20944/preprints202505.0100.v1

Experimental results (see Figure 8 a) show different film solubilities in water depending on the concentration of PVA and protein. In general, as the concentration of PVA increases, a progressive decrease in film solubility is observed, and a decrease in the standard deviation related to inhomogeneity in film structure. This behaviour reflects both the higher solubility of BSF protein compared to PVA and a structural transition of the material from an amorphous to a more crystalline configuration that is less accessible to water [48]. The decrease in the PVA crystallinity correlated with the increase of protein concentration in films was demonstrated by previous DSC analysis.

3.6. Water Uptake

Analysis of water uptake curves (see Figure 8b) shows a significant increase in water uptake in the first eight hours for all the PVA/BSF protein films analyzed, followed by a gradual slowdown leading to a plateau within 24 h.

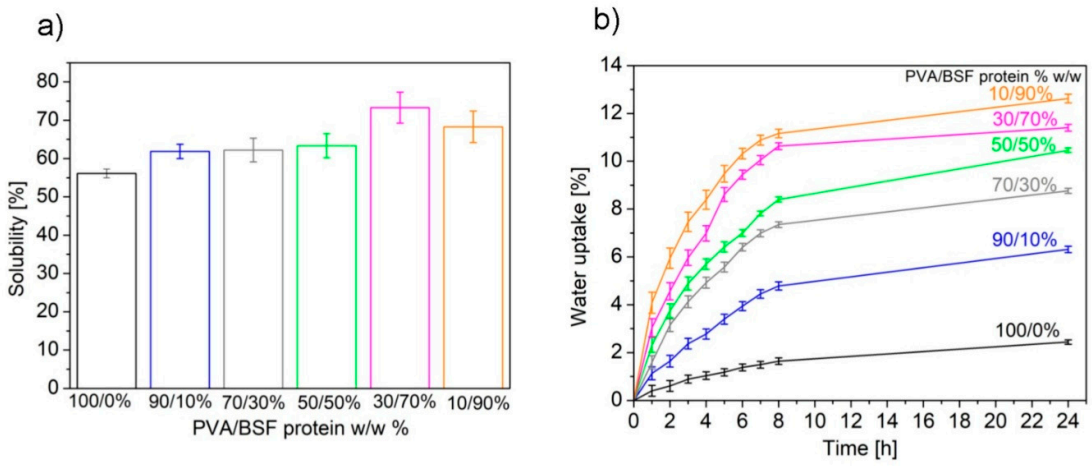

Figure 8. Solubility in water (a) and water uptake (b) of PVA/BSF protein films at different concentration .

Films with a high concentration of PVA show consistently lower water uptake values at each time step. This behavior is attributable to the crystalline structure of PVA, which organizes its polymer chains into ordered and compact configurations, reducing the space available for water molecules and limiting the mobility of polymer chains that further hinder water uptake. In addition, the low standard deviation observed in these samples suggests homogeneous and predictable behavior due to the uniform distribution of PVA within the material. In contrast, films with higher protein concentrations exhibit significantly higher water uptake. Proteins, predominantly amorphous, offer more hydrophilic sites, such as amine and carboxyl groups, which can form hydrogen bonds with water. This disordered structure promotes rapid absorption in the early stages and a greater ability to retain moisture. In addition, the data show greater variability in samples with high protein content, which can be attributed to local inhomogeneities in protein distribution.

3.7. Morphological Characterization

Figure 9 shows the surfaces of the PVA/BSF protein films at different concentrations at 100 x magnification.

For the pure PVA film, the surface appears smooth and homogeneous, confirming that the material forms an isotropic and stable matrix. At 10 % protein addition, slight inhomogeneities emerge, but no porosity is detected and the polymer matrix retains its cohesion. Increasing the protein amount, small, randomly distributed cracks begin to appear, and some areas of the film appear darker, suggesting the presence of microvoids or areas of reduced density, given the onset of phase separation between PVA and BSF protein. In PVA/BSF 30/70% w/w protein films, the surface is

 doi:10.20944/preprints202505.0100.v1

characterized by a network of interconnected cracks, making the material less resistant to mechanical stress. In PVA/BSF 10/90% w/w protein films, proteins aggregate and don't integrate properly with the remaining PVA. Moreover, film porosity is very pronounced, and the uneven distribution of proteins creates weak points that promote fracture formation. Finally, the neat protein film shows separate fragments. Analogous results were obtained by Rajabinejad et al. in similar materials [49].

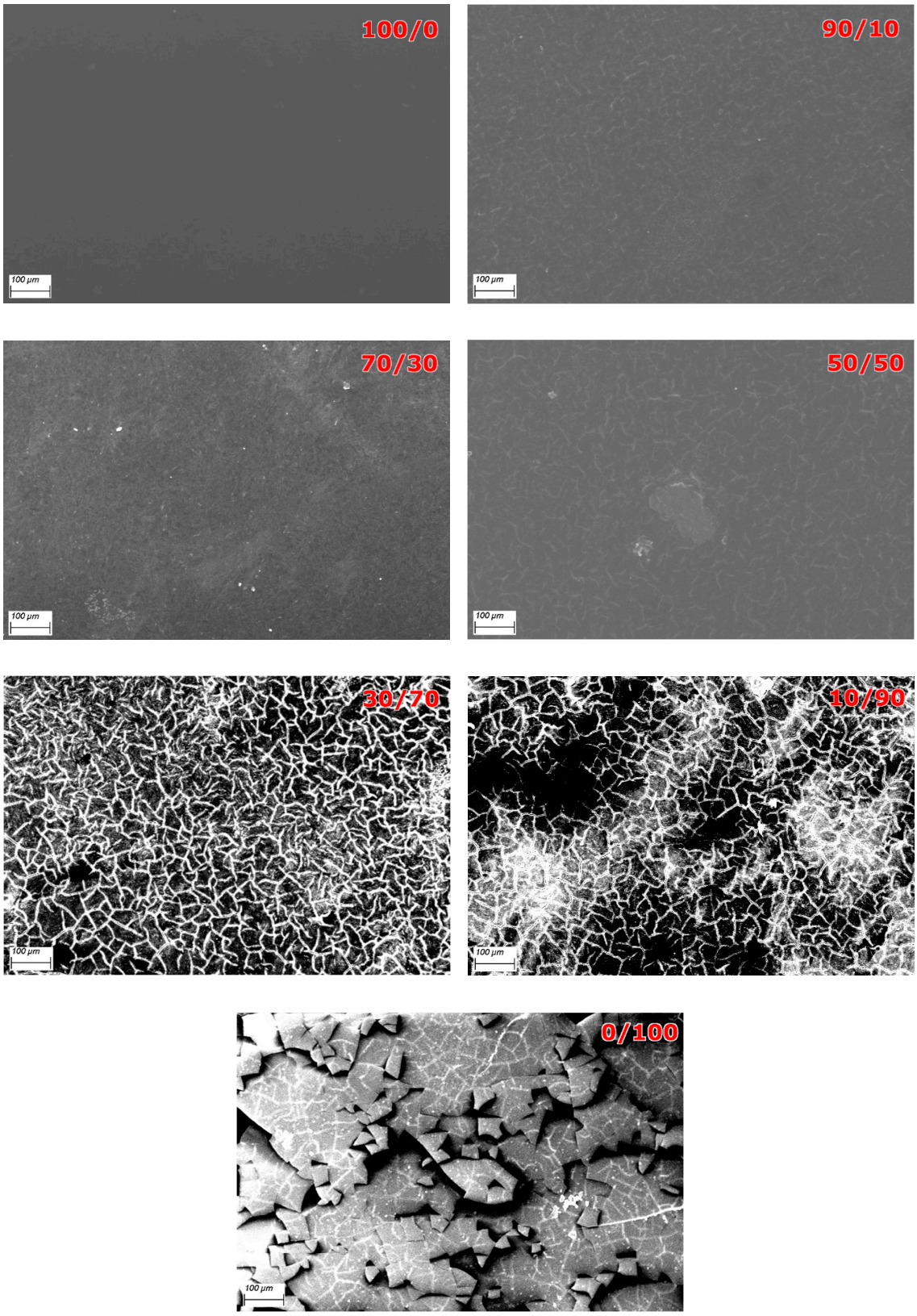

 doi:10.20944/preprints202505.0100.v1

Figure 9. SEM pictures at 100X of PVA/BSF protein films at different concentration 100/0, 90/10, 70/30, 50/50, 30/70, 10/90 and 0/100 (% w/w).

3.8. Tensile Behaviour

The tensile mechanical properties of the films at different PVA/BSF protein concentrations are summarized in Table 3. For pure PVA films, the tensile strength of 9.39 MPa is attributable to the uniform and stable crystal structure of PVA, which ensures a homogeneous distribution of mechanical stress. By introducing protein, the tensile strength first slowly decreases until 50/50% w/w PVA/ BSF protein suggesting that protein acts as a plasticizer, promoting a balanced stress distribution and stability of the crystalline network. Increasing the amount of protein until 70% w/w, however, the tensile strength decreases strongly as the crystalline network appears to be compromised by protein dominance. As the amount of protein increases, the elongation at break gradually increases. In particular, for the neat PVA film, the elongation at the break is 50.90 %, reflecting the moderate ductility of this polymer because the crystalline network restricts the sliding of polymer chains. Adding 10 % protein, the film strain rises slightly, suggesting an onset of plasticization that reduces the material's stiffness. As the protein content increases, the strain increases more and more, reaching 209.99 % with 30% PVA, due to the increased mobility of the polymer chains that makes the material increasingly ductile. Similar results were obtained by Silva et al. in PVA and gelatin films [48]. Finally, from Table 3 it can be seen that the modulus gradually decreases as the amount of PVA decreases.

Table 3. Tensile strength, elongation at break and modulus of PVA/BSF protein films at different concentration.

PVA/BSF protein [%w/w]	Tensile strength [MPa]	Elongation at break [%]	Modulus [GPa]
100/0	9.39	50.90	6.66
90/10	7.52	56.79	2.59
70/30	9.16	98.99	2.21
50/50	7.78	190.06	1.39
30/70	4.51	209.99	1.33

3.9. Contact Angle

From Table 4, it can be seen that as the percentage of protein increases, the contact angle decreases from 67.6 ± 0.41° of pure PVA to 53.7 ± 0.95° of PVA/BSF protein 30/70% w/w, indicating greater film hydrophilicity. In addition, the standard deviation becomes more and more pronounced due to the increasingly irregular surface. Pure PVA film has hydrophilic functional groups; however, in the crystalline component, the denser packing of polymer chains limits exposure of hydrophilic groups, which has a direct impact on the wettability properties of the material. In films with 90% PVA, the proteins introduce polar groups that promote hydrogen bonds with water. Although PVA remains predominant, it maintains some resistance to liquid diffusion. As protein content increases, the contact angle decreases further due to protein functional groups facilitating interaction with water molecules. In addition, the increase in hydrophilicity as the protein amount increases could be related to the roughness of the films, as shown by SEM images [50].

Table 4. Contact angle values of PVA/BSF protein films at different concentration.

PVA/BSF protein [%w/w]	Contact angle
100/0	67.6 ± 0.41°
90/10	65.6 ± 0.54°
70/30	59.7 ± 0.67°
50/50	56.1 ± 0.80°

 doi:10.20944/preprints202505.0100.v1

30/70	53.7 ± 0.95°

3.10. Biodegradation Testing in Soil

Figure 10 summarizes the weight losses of PVA/BSF protein films at different concentrations after 10, 20, 30, 60 and 90 days of burial in soil.

The curves show that samples with a higher protein content degrade more rapidly, while films with a higher percentage of PVA are more resistant to soil degradation. The degradation is generally characterized by a rapid initial mass loss, followed by a gradual slowdown. The pure PVA film shows a weight loss of 12% w/w after 90 days, confirming poor biodegradability in the soil as confirmed by other authors [51] because few microorganisms present in the soil can biodegrade PVA [52]. As the percentage of protein increases the sample weight loss increases until 80% w/w after 90 days of soil burial for the 30/70% w/w PVA/BSF protein sample. Lowering and disappearance of the Amide I (1650 cm^{-1}) and Amide II (1550 cm^{-1}) absorption peaks in FTIR spectra of biodegraded films (data not shown) highlight that the proteins are degraded in soil faster than PVA. This behaviour of rapid protein degradation in soil is confirmed by Dani et al. [53].

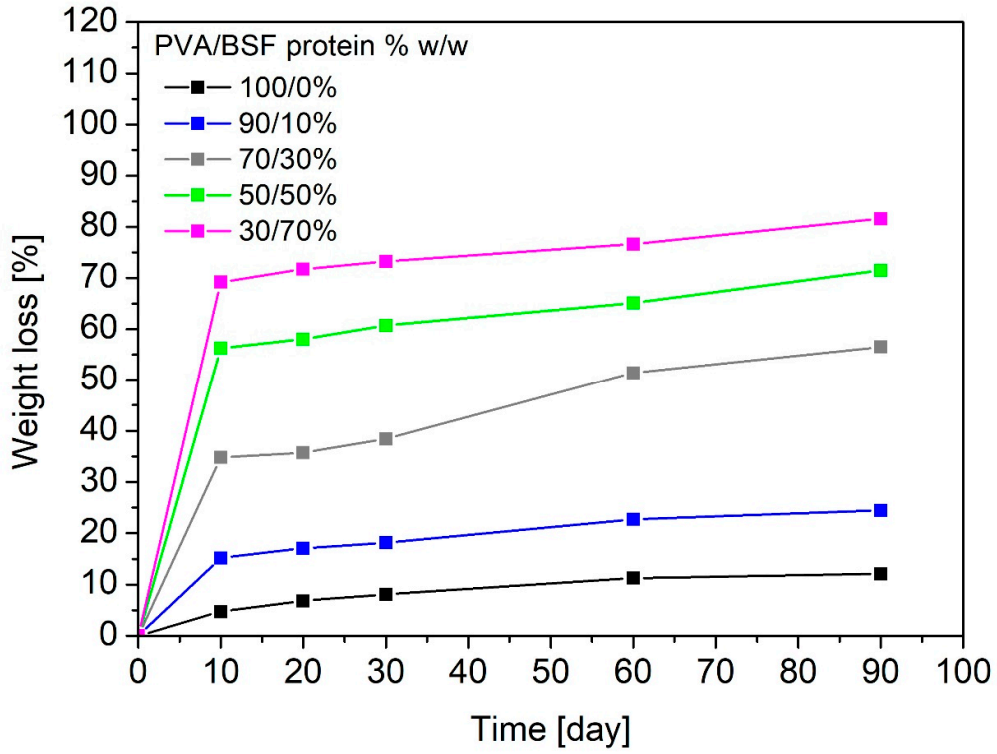

Figure 10. Weight loss of PVA/BSF protein films with different compositions after 10, 20, 30, 60, 90 days of burial in the soil.

4. Conclusions

Proteins extracted from BSF larvae with superheated water without harsh chemical reagents were mixed with PVA to obtain bioplastics with properties that can be modulated according to different proportions of PVA and BSF proteins. FTIR analysis showed the formation of hydrogen bonds that ensure good cohesion of the polymer matrix, suggesting good compatibility between the two components. However, a nonuniform distribution of proteins within the polymer matrix is shown, with a tendency for aggregate formation affecting the material's mechanical properties with decreased tensile strength and increased deformability in films with high protein content. This behaviour suggests that proteins act as plasticizers in the films. Thermal analyses showed that the

 doi:10.20944/preprints202505.0100.v1

films exhibit lower thermal stability with increasing protein content due to amorphous proteins interfering with the crystallinity of PVA. In addition, films with higher protein content show higher water uptake, water solubility, hydrophilicity, and biodegradation faster in soil than films with higher PVA content. PVA/BSF protein bioplastics can be used as biodegradable packaging or as agricultural mulches as a sustainable alternative to traditional plastic materials like LDPE, which are a source of pollution due to fragmentation and persistence in soil. These bioplastics, in addition to protecting the soil, also act as fertilizers as the film degradation releases nutrients such as organic carbon and nitrogen in the soil [54].

Author Contributions: Conceptualization, M.Z. and S.DV.; Methodology, A.M. and G.DF.; Investigation, A. DP., G. DF and A.A.; Resources, M.Z.; Data Curation, G. DF. and A.A.; Writing – Original Draft Preparation, M.Z. and A. DP.; Writing – Review & Editing, A.M. and S. DV.; Supervision, S. DV.; Funding Acquisition, M.Z. All authors have read and agreed to the published version of the manuscript.

Funding: The research was funded by the research project HI-Tech "Hermetia illucens biofactory: from waste to high-value technological products", PRIN 2022 (D.D. MUR n.104 del 02/02/2022).

References

1. Caligiani, A.; Marseglia, A.; Leni, G.; Baldassarre, S.; Maistrello, L.; Dossena, A.; Sforza, S. Composition of Black Soldier Fly Prepupae and Systematic Approaches for Extraction and Fractionation of Proteins, Lipids and Chitin. Food Res. Int. 2018, 105, 812–820, doi:10.1016/J.FOODRES.2017.12.012.
2. Edea, C.; Tesfaye, E.; Yirgu, T.; Alewi, M. Black Soldier Fly (Hermetia Illucens) Larvae as a Sustainable Source of Protein in Poultry Feeding: A Review. *Ethiop. J. Agric. Sci.* **2022**, *32*, 89–104.
3. Nguyen, T.-X.; Tomberlin, J.; Vanlaerhoven, S. Ability of Black Soldier Fly (Diptera: Stratiomyidae) Larvae to Recycle Food Waste. *Environ. Entomol.* **2015**, *44*, 406–410, doi:10.1093/ee/nvv002.
4. Van Huis, A.; Gasco, L. Insects as Feed for Livestock Production. *Science (80-.).* **2023**, *379*, 138–139, doi:10.1126/science.adc9165.
5. Odongo, E.E.; Bbosa, W.K.; Kahunde, P.K. Black Soldier Fly (BSF): A Sustainable Solution for Protein, Waste Management, and a Circular Bio-Economy. *Eur. J. Theor. Appl. Sci.* **2024**, *2*, 822–834, doi:10.59324/ejtas.2024.2(3).64.
6. Regulation (EC) No 1069/2009 of the European Parliament and of the Council of 21 October 2009 Laying down Health Rules as Regards Animal by-Products and Derived Products Not Intended for Human Consumption and Repealing Regulation (EC) No 1774/2002. Available online: https://eur-lex.europa.eu/eli/reg/2009/1069/oj/eng.
7. Commission Regulation (EU) 2017/1017 of 15 June 2017 Amending Regulation (EU) No 68/2013 on the Catalogue of Feed Materials (Text with EEA Relevance.).
8. IPIFF Vision Paper on the Future of the Insect Sector towards 2030. The European Insect Sector Today: Challenges, Opportunities and Regulatory Landscape. Available online: https://ipiff.org/ipiff-vision-paper/ (accessed on 7 March 2022).
9. Fowles, T.M.; Nansen, C. Insect-Based Bioconversion: Value from Food Waste BT - Food Waste Management: Solving the Wicked Problem. In; Närvänen, E., Mesiranta, N., Mattila, M., Heikkinen, A., Eds.; Springer International Publishing: Cham, 2020; pp. 321–346 ISBN 978-3-030-20561-4.
10. Ravi, H.K.; Degrou, A.; Costil, J.; Trespeuch, C.; Chemat, F.; Vian, M.A. Larvae Mediated Valorization of Industrial, Agriculture and Food Wastes: Biorefinery Concept through Bioconversion, Processes, Procedures, and Products. *Processes* **2020**, *8*, 857, doi:10.3390/pr8070857.
11. Shaboon, A.M.; Qi, X.; Omar, M.A.A. Insect-Mediated Waste Conversion BT - Waste-to-Energy: Recent Developments and Future Perspectives towards Circular Economy. In; Abomohra, A.E.-F., Wang, Q., Huang, J., Eds.; Springer International Publishing: Cham, 2022; pp. 479–509 ISBN 978-3-030-91570-4.
12. Ragossnig, H.A.; Ragossnig, A.M. Biowaste Treatment through Industrial Insect Farms: One Bioeconomy Puzzle Piece towards a Sustainable Net-Zero Carbon Economy? *Waste Manag. Res. J. a Sustain. Circ. Econ.* **2021**, *39*, 1005–1006, doi:10.1177/0734242X211036949.

 doi:10.20944/preprints202505.0100.v1

13. Siddiqui, S.A.; Ristow, B.; Rahayu, T.; Putra, N.S.; Widya Yuwono, N.; Nisa', K.; Mategeko, B.; Smetana, S.; Saki, M.; Nawaz, A.; et al. Black Soldier Fly Larvae (BSFL) and Their Affinity for Organic Waste Processing. *Waste Manag.* **2022**, *140*, 1–13, doi:https://doi.org/10.1016/j.wasman.2021.12.044.
14. Eurostat 2024 Available online: https://ec.europa.eu/eurostat/web/products-eurostat-news/w/ddn-20240927-2#:~:text=In 2022%2C around 132 kilogrammes,of 72 kg per inhabitant.
15. Nayak, A.; Bhushan, B. An Overview of the Recent Trends on the Waste Valorization Techniques for Food Wastes. *J. Environ. Manage.* **2019**, *233*, 352–370, doi:https://doi.org/10.1016/j.jenvman.2018.12.041.
16. Smets, R.; Verbinnen, B.; Van De Voorde, I.; Aerts, G.; Claes, J.; Van Der Borght, M. Sequential Extraction and Characterisation of Lipids, Proteins, and Chitin from Black Soldier Fly (Hermetia Illucens) Larvae, Prepupae, and Pupae. *Waste and Biomass Valorization* **2020**, *11*, 6455–6466, doi:10.1007/s12649-019-00924-2.
17. Martín-López, H.; Ayora-Talavera, T.; Liedo, P.; Ramos-Díaz, A.; Herrera-Rodríguez, S.; Cuevas-Bernardino, J.C.; Pacheco, N. The Mexican Fruit Fly Puparia (Anastrepha Ludens) and the Black Soldier Fly Imagoes (Hermetia Illucens), Promising Alternative Sources of Chitin. *MRS Adv.* **2024**, *9*, 1747–1753, doi:10.1557/s43580-024-01008-7.
18. Ai, H.; Wang, F.; Yang, Q.; Zhu, F.; Lei, C. Preparation and Biological Activities of Chitosan from the Larvae of Housefly, Musca Domestica. *Carbohydr. Polym.* **2008**, *72*, 419–423, doi:https://doi.org/10.1016/j.carbpol.2007.09.010.
19. Batish, I.; Brits, D.; Valencia, P.; Miyai, C.; Rafeeq, S.; Xu, Y.; Galanopoulos, M.; Sismour, E.; Ovissipour, R. Effects of Enzymatic Hydrolysis on the Functional Properties, Antioxidant Activity and Protein Structure of Black Soldier Fly (Hermetia Illucens) Protein. *Insects* **2020**, *11*, 876, doi:10.3390/insects11120876.
20. McNeil, S.J.; Sunderland, M.R.; Zaitseva, L.I. Closed-Loop Wool Carpet Recycling. *Resour. Conserv. Recycl.* **2007**, *51*, 220–224, doi:10.1016/j.resconrec.2006.09.006.
21. Zoccola, M.; Montarsolo, A.; Mossotti, R.; Patrucco, A.; Tonin, C. Green Hydrolysis as an Emerging Technology to Turn Wool Waste into Organic Nitrogen Fertilizer. *Waste and Biomass Valorization* **2015**, *6*, 891–897, doi:10.1007/s12649-015-9393-0.
22. Bhavsar, P.; Patrucco, A.; Montarsolo, A.; Mossotti, R.; Rovero, G.; Giansetti, M.; Tonin, C. Superheated Water Hydrolysis of Waste Wool in a Semi-Industrial Reactor to Obtain Nitrogen Fertilizers. *ACS Sustain. Chem. Eng.* **2016**, *4*, doi:10.1021/acssuschemeng.6b01664.
23. Yin, J.; Rastogi, S.; Terry, A.E.; Popescu, C. Self-Organization of Oligopeptides Obtained on Dissolution of Feather Keratins in Superheated Water. *Biomacromolecules* **2007**, *8*, 800–806, doi:10.1021/bm060811g.
24. Bhavsar, P.; Dalla Fontana, G.; Tonin, C.; Patrucco, A.; Zoccola, M. Superheated Water Hydrolyses of Waste Silkworm Pupae Protein Hydrolysate: A Novel Application for Natural Dyeing of Silk Fabric. *Dye. Pigment.* **2020**, *183*, 108678, doi:https://doi.org/10.1016/j.dyepig.2020.108678.
25. Bhavsar, P.S.; Dalla Fontana, G.; Zoccola, M. Sustainable Superheated Water Hydrolysis of Black Soldier Fly Exuviae for Chitin Extraction and Use of the Obtained Chitosan in the Textile Field. *ACS Omega* **2021**, *6*, 8884–8893, doi:10.1021/acsomega.0c06040.
26. Caringella, R.; Bhavsar, P.; Dalla Fontana, G.; Patrucco, A.; Tonin, C.; Pozzo, P.D.; Zoccola, M. Fabrication and Properties of Keratoses/Sericin Blend Films. *Polym. Bull.* **2022**, *79*, 2189–2204, doi:10.1007/s00289-021-03620-1.
27. Bonilla, J.; Fortunati, E.; Atarés, L.; Chiralt, A.; Kenny, J.M. Physical, Structural and Antimicrobial Properties of Poly Vinyl Alcohol–Chitosan Biodegradable Films. *Food Hydrocoll.* **2014**, *35*, 463–470, doi:https://doi.org/10.1016/j.foodhyd.2013.07.002.
28. Rajabinejad, H.; Zoccola, M.; Patrucco, A.; Montarsolo, A.; Chen, Y.; Ferri, A.; Muresan, A.; Tonin, C. Fabrication and Properties of Keratoses/Polyvinyl Alcohol Blend Films. *Polym. Bull.* **2020**, *77*, 3033–3046, doi:10.1007/s00289-019-02889-7.
29. Dou, Y.; Zhang, B.; He, M.; Yin, G.; Cui, Y.; Savina, I.N. Keratin/Polyvinyl Alcohol Blend Films Cross-Linked by Dialdehyde Starch and Their Potential Application for Drug Release. *Polymers (Basel).* **2015**, *7*, 580–591, doi:10.3390/polym7030580.
30. Limpan, N.; Prodpran, T.; Benjakul, S.; Prasarpran, S. Influences of Degree of Hydrolysis and Molecular Weight of Poly(Vinyl Alcohol) (PVA) on Properties of Fish Myofibrillar Protein/PVA Blend Films. *Food Hydrocoll.* **2012**, *29*, 226–233, doi:https://doi.org/10.1016/j.foodhyd.2012.03.007.

 doi:10.20944/preprints202505.0100.v1

31. Costa, A.; Encarnação, T.; Tavares, R.; Todo Bom, T.; Mateus, A. Bioplastics: Innovation for Green Transition. *Polymers (Basel).* **2023**, *15*, doi:10.3390/polym15030517.
32. Asgher, M.; Qamar, S.A.; Bilal, M.; Iqbal, H.M.N. Bio-Based Active Food Packaging Materials: Sustainable Alternative to Conventional Petrochemical-Based Packaging Materials. *Food Res. Int.* **2020**, *137*, 109625, doi:https://doi.org/10.1016/j.foodres.2020.109625.
33. *Bioplastics for Sustainable Development*; Kuddus, M., Roohi, Eds.; Springer Singapore: Singapore, 2021; ISBN 978-981-16-1822-2.
34. Tian, L.; Jinjin, C.; Ji, R.; Ma, Y.; Yu, X. Microplastics in Agricultural Soils: Sources, Effects, and Their Fate. *Curr. Opin. Environ. Sci. Heal.* **2022**, *25*, 100311, doi:https://doi.org/10.1016/j.coesh.2021.100311.
35. Bhavsar, P.; Balan, T.; Dalla Fontana, G.; Zoccola, M.; Patrucco, A.; Tonin, C. Sustainably Processed Waste Wool Fiber-Reinforced Biocomposites for Agriculture and Packaging Applications. *Fibers* **2021**, *9*, doi:10.3390/fib9090055.
36. Setti, L.; Francia, E.; Pulvirenti, A.; De Leo, R.; Martinelli, S.; Maistrello, L.; Macavei, L.I.; Montorsi, M.; Barbi, S.; Ronga, D. Bioplastic Film from Black Soldier Fly Prepupae Proteins Used as Mulch: Preliminary Results. *Agronomy* **2020**, *10*, doi:10.3390/agronomy10070933.
37. GONTARD, N.; GUILBERT, S.; CUQ, J.-L. Edible Wheat Gluten Films: Influence of the Main Process Variables on Film Properties Using Response Surface Methodology. *J. Food Sci.* **1992**, *57*, 190–195, doi:https://doi.org/10.1111/j.1365-2621.1992.tb05453.x.
38. Patrucco, A.; Zoccola, M.; Consonni, R.; Tonin, C. Wool Cortical Cell-Based Porous Films. *Text. Res. J.* **2013**, *83*, 1563–1573, doi:10.1177/0040517512458342.
39. EN-ISO 5079 (1995) Determination of Breaking Force and Elongation at Break of Individual Fbers. Int Stand Organ. **1995**.
40. Queiroz, L.S.; Regnard, M.; Jessen, F.; Mohammadifar, M.A.; Sloth, J.J.; Petersen, H.O.; Ajalloueian, F.; Brouzes, C.M.C.; Fraihi, W.; Fallquist, H.; et al. Physico-Chemical and Colloidal Properties of Protein Extracted from Black Soldier Fly (Hermetia Illucens) Larvae. *Int. J. Biol. Macromol.* **2021**, *186*, 714–723, doi:https://doi.org/10.1016/j.ijbiomac.2021.07.081.
41. Mahmood, T.; Malik, M.; Bano, A.; Umer, J.; Shaheen, A. Nanocatalytic Conversion of Waste Palm Oil Grade III and Poplar Plant's Wood Sawdust into Fuel. *Innov. Energy Res.* **2017**, *06*, doi:10.4172/2576-1463.1000170.
42. Tinti, A.; Tugnoli, V.; Bonora, S.; Francioso, O. Recent Applications of Vibrational Mid-Infrared (IR) Spectroscopy for Studying Soil Components: A Review. *J. Cent. Eur. Agric.* **2015**, *16*, 1–22, doi:10.5513/JCEA01/16.1.1535.
43. Gou, M.X.; Yang, X.H. Preparation and Characterization of Wool Keratin/PVA Blended Films. *Adv. Mater. Res.* **2011**, *175–176*, 132–136, doi:10.4028/www.scientific.net/AMR.175-176.132.
44. Mansur, H.S.; Sadahira, C.M.; Souza, A.N.; Mansur, A.A.P. FTIR Spectroscopy Characterization of Poly (Vinyl Alcohol) Hydrogel with Different Hydrolysis Degree and Chemically Crosslinked with Glutaraldehyde. *Mater. Sci. Eng. C* **2008**, *28*, 539–548, doi:https://doi.org/10.1016/j.msec.2007.10.088.
45. Hyder, M.N.; Huang, R.Y.M.; Chen, P. Correlation of Physicochemical Characteristics with Pervaporation Performance of Poly(Vinyl Alcohol) Membranes. *J. Memb. Sci.* **2006**, *283*, 281–290, doi:https://doi.org/10.1016/j.memsci.2006.06.045.
46. Nakano, Y.; Bin, Y.; Bando, M.; Nakashima, T.; Okuno, T.; Kurosu, H.; Matsuo, M. Structure and Mechanical Properties of Chitosan/Poly(Vinyl Alcohol) Blend Films. *Macromol. Symp.* **2007**, *258*, 63–81, doi:https://doi.org/10.1002/masy.200751208.
47. Mshayisa, V.V.; Van Wyk, J.; Zozo, B.; Rodríguez, S.D. Structural Properties of Native and Conjugated Black Soldier Fly (Hermetia Illucens) Larvae Protein via Maillard Reaction and Classification by SIMCA. *Heliyon* **2021**, *7*, e07242, doi:10.1016/j.heliyon.2021.e07242.
48. Silva, G.G.D.; Sobral, P.J.A.; Carvalho, R.A.; Bergo, P.V.A.; Mendieta-Taboada, O.; Habitante, A.M.Q.B. Biodegradable Films Based on Blends of Gelatin and Poly (Vinyl Alcohol): Effect of PVA Type or Concentration on Some Physical Properties of Films. *J. Polym. Environ.* **2008**, *16*, 276–285, doi:10.1007/s10924-008-0112-9.

 doi:10.20944/preprints202505.0100.v1

49. Rajabinejad, H.; Zoccola, M.; Patrucco, A.; Montarsolo, A.; Chen, Y.; Ferri, A.; Muresan, A.; Tonin, C. Fabrication and Properties of Keratoses/Polyvinyl Alcohol Blend Films. *Polym. Bull.* **2020**, *77*, 3033–3046, doi:10.1007/s00289-019-02889-7.
50. Jayasekara, R.; Harding, I.; Bowater, I.; Christie, G.B..; Lonergan, G.. Preparation, Surface Modification and Characterisation of Solution Cast Starch PVA Blended Films. *Polym. Test.* **2004**, *23*, 17–27, doi:10.1016/S0142-9418(03)00049-7.
51. Chiellini, E.; Corti, A.; D'Antone, S.; Solaro, R. Biodegradation of Poly (Vinyl Alcohol) Based Materials. *Prog. Polym. Sci.* **2003**, *28*, 963–1014, doi:10.1016/S0079-6700(02)00149-1.
52. Ishigaki, T.; Kawagoshi, Y.; Ike, M.; Fujita, M. Biodegradation of a Polyvinyl Alcohol-Starch Blend Plastic Film. *World J. Microbiol. Biotechnol.* **1999**, *15*, 321–327, doi:10.1023/A:1008919218289.
53. Jagadeesh, D.; Jeevan Pradsad Reddy, D.; Varada Rajulu, A.; Li, R. Green Composites from Wheat Protein Isolate and Hildegardia Populifolia Natural Fabric. *Polym. Compos.* **2011**, *32*, 398–406, doi:https://doi.org/10.1002/pc.21055.
54. Barbi, S.; Spinelli, R.; Ferrari, A.M.; Montorsi, M. Design and Environmentale Assessment of Bioplastics from Hermetia Illucens Prepupae Proteins. *Environ. Eng. Manag. J.* **2019**, *18*, 2123–2131.